Mechanical Stability of PV Modules

Analyses of the Influence of the Glass Quality

Jochen Markert[1] ID, Frank Ensslen[1] ID, Tobias Rist[2] ID, Andreas J. Beinert[1] ID, Enzo Job[1] ID,
Ingrid Hädrich[1] ID, and Daniel Philipp[1] ID

[1] Fraunhofer Institute for Solar Energy Systems ISE, Freiburg, Germany

[2] Fraunhofer Institute for Mechanics of Materials IWM, Freiburg, Germany

Abstract. A significant increase of reported glass breakages in the field was recognized during the past three years, where a disproportionately high number of modules were affected by glass breakage. Different substructures and module designs are affected, framed and unframed modules, tracked and fixed systems. What all inquiries have in common, however, is that modules with a double-glazed design with ≤ 2.5 mm glass thickness are affected and the problems were observed after just a few months of field operation. Various factors such as heavy weather events, faulty installation or errors in the structural design could be excluded as root causes and our experience points on additional, more fundamental problems that are associated in particular with the continuing trend towards larger modules > 3 m^2 and thinner module glass ≤ 2mm [1]. Furthermore, it seems that the residual compressive surface stress of the glass as one major parameter that determines the stability of glass panes has not been considered in this context in the PV module industry yet. In this work, we focus on the glass thickness in combination with the compressive surface stress. Besides qualitative methods, one possibility to investigate the surface stress quantitatively was a scattered light polariscope (SCALP), previously used in the glass industry. In particular, the aim was to validate the SCALP measurement method for the use on PV modules. Furthermore, a potential correlation between the surface compressive stress and the mechanical stability of various common module designs with 2.0 mm and 1.6 mm glass was investigated.

Keywords: PV Module Reliability, Glass Breakage, Mechanical Stability, Glass Surface Stress, Bending Strength

1. Introduction

Glass is a central component in the design of PV modules, since it represents an inert material with low diffusivity and a high mechanical strength. Especially in glass/glass designs, the trend is going towards module formats approaching 3 m^2 and larger, while the glass thickness is reduced to ≤ 2.0 mm, which appears to be a contradictory development regarding the stability of PV modules in general [1]. This determination is supported by significantly increased numbers of PV modules showing glass breakages reported from power plants from all over the world during the past 3 years. In contrast to previous reports about glass breakages [2–5], current cases occur after a relatively short time (up to one year) after installation and common root causes for instance extreme weather events, installation errors, transporting damages and hot-spots can be excluded.

Besides surface defects and the edge quality, the residual surface compressive stress introduced during the tempering process is one of the major parameters determining the glass

stability in general. However, in contrast to the glass industry, where the glass quality is determined with statistical evaluation of mechanical tests (four-point-bending- [6] or double-ring-bending test [7]) the assessment in PV laminates was up to now limited to a qualitative evaluation of breakage patterns. Observations during investigations already suggested that the glass quality used in the failed modules is generally lower than the one from previously module standard designs with 3.2 mm thermally toughened safety glass (TTG).
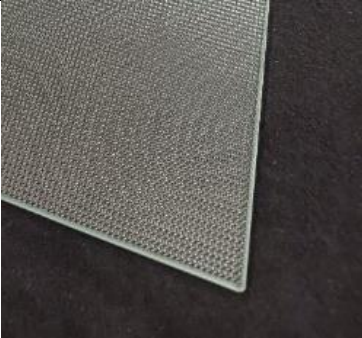
One technique to determine the residual surface compressive stress quantitatively is a scattered light polariscope (SCALP). In the scope of this work, the SCALP method was validated for measurements on PV modules, starting with a comprehensive study on glass samples with known glass qualities. Furthermore, the SCALP measurements are correlated with results from a double-ring-bending test conducted at Fraunhofer IWM. In addition, four different commercially available PV module types with different glass thicknesses were investigated with the SCALP. Subsequently, the modules were subject to a mechanical load (ML) test until failure and the results were correlated with the surface compressive stresses measured with SCALP.

2. Tests on Glass Samples

2.1. Sample Description

Sets of four different glass types with known degrees of prestressing were used (Table 1). Each set included a total of 30 samples.

Table 1. Types of investigated glass samples.

Glass Qualities	Visual Appearance
Float glass (Float) acc. to EN 572-2 Thickness 3 mm	
Heat strengthened glass (HSG) acc. to EN 1863-1 Thickness 4 mm	
Thermally toughened safety glass (TTG) acc. to EN 12150-1 Thickness 3 mm	Flat glass
HSG acc. to EN 1863-1, textured Thickness 4 mm	Textured glass

Furthermore, one solar glass pane (TTG acc. to EN 12150-1, thickness 3.2 mm) with one coated und one uncoated side was used to investigate the influence of an anti-reflection coating (ARC) on the results of the SCALP measurements.

2.2. Methodology

The residual surface compressive stress was measured with a SCALP-05 from GlasStress OÜ (Lituania). The method includes laser light, which is coupled into the glass with a defined angle, typically around 45°. Differences in the glass stress with increasing depth result in a rotation of the polarization plane and consequently a reduction in scattering intensity orthogonal to the initial polarization plane. A camera positioned orthogonally to the layer beam and downward on the glass surface records the intensity difference in scattered light, which can be recalculated into a stress profile. The minimum measurement depth according to the manufacturer is 1 mm. All samples investigated were within the measurement range of the device. Prior to each measurement series, the function of the device was checked with a reference sample from the manufacturer, consisting of a glass pane with a defined measurement point and known value for the surface compressive stress.

To determine the fracture stress of the glass with edge defects excluded, each sample was subject to a double-ring bending test based on EN 1288-5 [7]. The tests were performed on a Instron 8090 testing machine (Figure 1). The standard defines that only fractures with origin under the load ring are considered for the evaluation. However, samples were also considered when the origin of fracture was in the range of r > 18 mm and r < 90 mm, because the fracture stress could be recalculated with a simulation model.
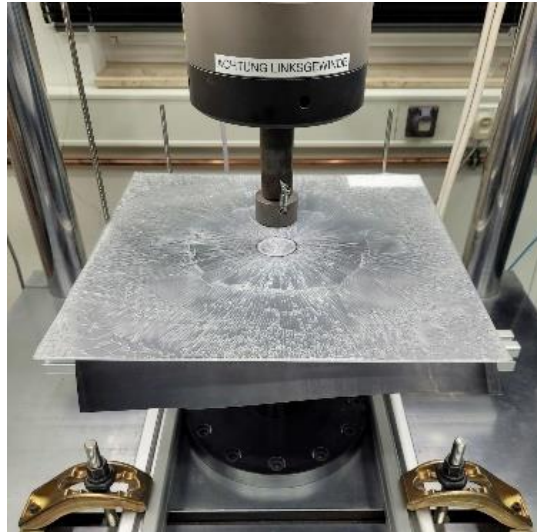

Figure 1. Double-ring bending test based on EN 1288-5 [7] conducted at Fraunhofer IWM.

2.3. Results

To qualify the SCALP method for the use on PV module glass, an initial investigation of glass samples with known glass qualities as defined in section 2.1. was conducted. Therefore, thirty samples of each type were measured with the SCALP in three positions (Figure 2, left). The results are shown in Figure 2 (right) with the grey areas, indicating literature value ranges for the surface compressive stress in HSG (-45 ±10 MPa) and TTG (≤ -90 MPa) [8]. Float showed an average residual surface stress of -2.7 ± 0.7 MPa, HSG of -56.1 ± 2.4 MPa, textured HSG of -46.7 ± 3.2 MPa and TTG of -116.1 ± 6.3 MPa. The results indicate that each of the sample type reaches the required minimum surface compressive stress for the respective glass quality. Furthermore, the surface tesxture in the glass showed only a slight influence on the measurement results with a reduction of approximately 10 MPa, mainly caused by an increase in the measurement uncertainty.
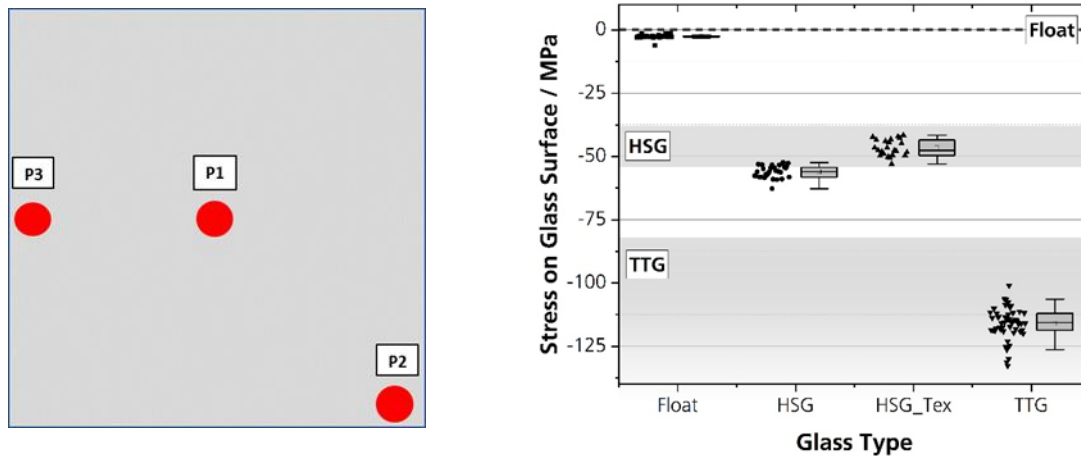
Figure 2. *Left: Sketch of SCALP measurement points on glass sample (30 x 30 cm^2); Right: Results of SCALP measurements on glass samples with different degrees of prestressing.*

The increasing scattering of the SCALP values with higher degrees of prestressing could be attributed to stress inhomogeneities introduced due to the complexity of the tempering process. By using a polarized light source behind, and a polarization filter acting as analyzer in front of the glass samples, the stress inhomogeneities in each glass type could be visualized as shown in Figure 3.

Figure 3. *Exemplary images of each sample type taken with a polarized light source behind and a polarization filter in front of the pane: Left: Float; Middle: HSG; Right: TTG.*

To correlate residual surface compressive stress with the fracture stress of the panes without the influence of edge defects, a double-ring-bending test based on DIN EN 1288-5 [7] was conducted on the same samples. The resulting bending strengths for each sample are shown in Figure 4 with mean values of 206 ±75 MPa (Float), 203 ± 34 MPa (HSG), 274 ± 70 MPa (HSG_Tex), and 335 ± 66 MPa (TTG). For each glass type the characteristic bending strengths (σ_k) for each glass type was calculated using the following equation 2.1 acc. to ISO 12491 [9]:

$$\sigma_k = \bar{x} - (k \times s) \qquad\qquad 2.1$$

With the mean value $\bar{x}$, a constant k dependent on the sample number defined in ISO 12491, Table 5, and the standard deviation s. The calculated values for the characteristic bending strengths were 60 MPa (Float), 137 MPa (HSG), 138 MPa (HSG_Tex), and 206 MPa (TTG).
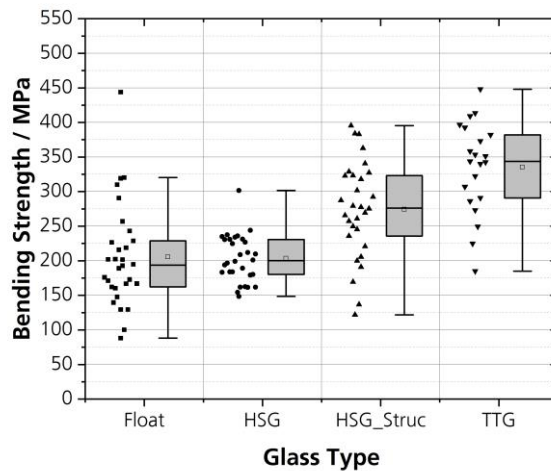
Figure 4. Bending strengths for each sample determined with a double-ring-bending test based on EN 1288-5.

Additionally, to investigate the influence of an anti-reflection coating (ARC), as it is typically used for solar front panes, a 3.2 mm solar glass (TTG acc. to EN 12150-1) with one coated and one uncoated side was measured at 15 points on each side as indicated in Figure 5 (left). The measurement results are shown in Figure 5 on the right side. Measurements on the ARC side resulted in -117.1 ± 6.2 MPa, while the non-coated side showed values of -127.4 ± 6.0 MPa. The results indicate that measurements through the ARC result in a slightly reduced value for the surface compressive stress. Here, the values for the coated side were used as a reference value for the stress measurements on the module front panes.
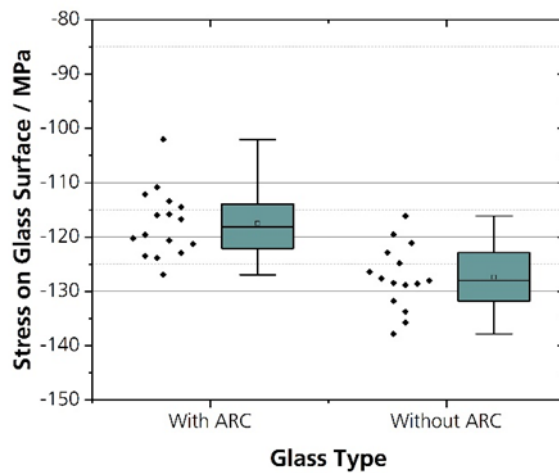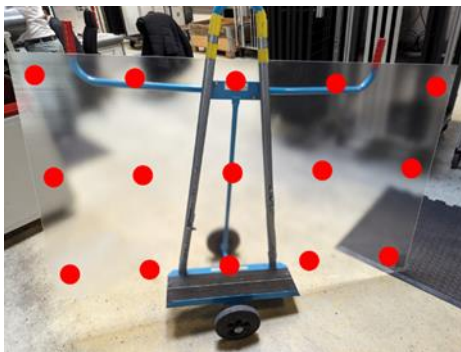

Figure 5. Left: Glass pane with one sided ARC coating and indicated positions of SCALP measurements (red points); Right: Residual surface stress on front (with ARC) and rear side (without ARC) of the pane.

3. Tests on PV Modules

3.1. Sample Description

For the tests on PV module level, four different commercially available module types with the specifications shown in Table 2 were used. To establish a minimum of statistics, five modules per type were measured.

Table 2. Types and number of investigated PV modules.

Module Type	Module area / mm²	Design	Glass thickness / mm	Frame height / mm	No. of Samples
1	1,722 x 1,134	Glass/glass	2.0 / 2.0	35	5
2	1,722 x 1,134	Glass/glass	1.6 / 1.6	30	5
3	1,762 x 1,134	Glass/glass	1.6 / 1.6	30	5
4	1,762 x 1,134	Glass/Back-sheet	3.2	30	5

3.2. Methodology

In order to determine the surface stress on PV module front panes, SCALP measurements were conducted as previously described in section 2.2.

In addition, load limits for PV modules were experimentally determined with a ML test stand from euroTECH Handling GmbH at Fraunhofer ISE in Freiburg. To reduce the influence of the clamp stability, the tests were conducted in pressure direction with a homogeneously applied surface load and a continuous load ramp of ~100 Pa/s until glass breakage occurred. The modules were mounted in a four-point fixation with clamps (width = 50 mm, torque = 15 Nm) at 20 % of the long module side and no cross braces to allow a free bending of the modules until failure. A representative module setup on the ML test stand is shown in Figure 6. The deflection was measured in the module center.
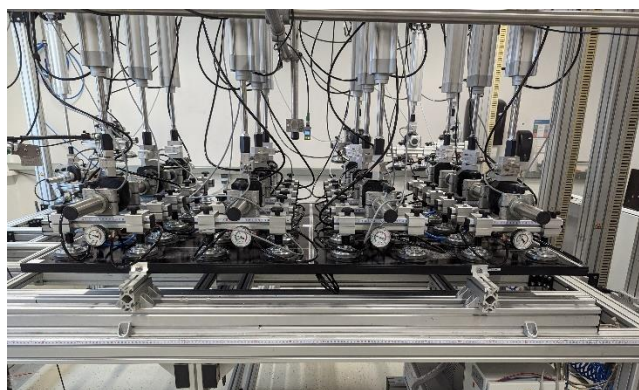

Figure 6. Representative module setup on the ML test stand for surface loads at Fraunhofer ISE.

3.3. Results

3.3.1. SCALP Measurements

Four commercially available PV module types (compare Table 2) were investigated (5 samples per type), beginning with measurements of the residual surface compressive stress, which was measured in four positions on each of the glass surfaces (front and rear) as shown in Figure 7 (left). Due to a highly reflective backsheet laminated below the glass and resulting secondary reflections, no measurements could be established on the rear side of module type 3. Module types 1 and 2 showed residual surface stresses on the rear side of 73.7 ± 5.3 MPa and -82.5 ± 5.0 MPa, respectively. The measurement results on the front panes with five samples per module type are shown in Figure 7 (right). The results showed measurable differences in the residual surface stress between the module types.
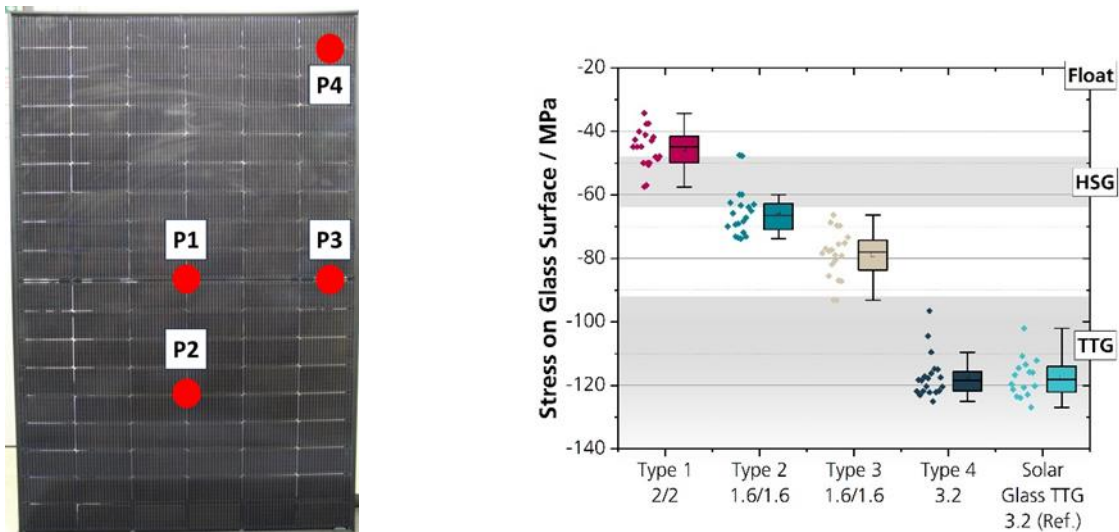

Figure 7. *Left: Exemplary module with measurement location for SCALP measurements (P1 – P4); Right: Results of the SCALP measurements on the module front pane of each module type and on the reference solar glass (TTG acc. to EN12150-1) with ARC.*

Module type 1 showed values of -45.6 ± 6.1 MPa, indicating surface stresses in the range of HSG. Type 2 and 3 showed values of -65.4 ± 7.5 MPa and -78.8 ± 7.6 MPa, ranging between HSG and TTG, while module type 4, with -117.2 ± 6.8 MPa showed values clearly in the range for TTG.

3.3.2. Mechanical Load Tests Until Failure

To correlate the SCALP measurements to a final module stability, the samples were subject to ML tests in pressure direction until failure with the specifications indicated in section 3.2. The results are shown in Figure 8.
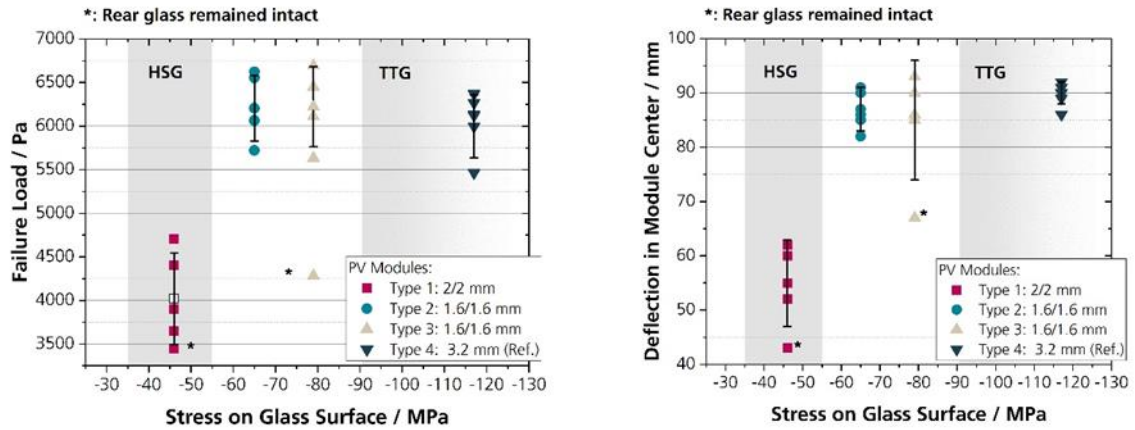
Figure 8. Results of the ML tests in pressure direction until failure on module types 1 to 4 (five samples per type); Left: Failure load vs. stress on glass surface; Right: Deflection vs. stress on glass surface.

Each module type was represented by five samples in total. Except of two modules (one of type 1 and one of type 3), which showed an intact rear pane after failure, all samples showed breakage of both panes - on front and rear side - as the dominant failure mode. Module type 1 resulted in an average failure load of 4,020 ± 520 Pa with a maximum deflection in the module center just before failure of 55 ± 8 mm. Within the five tested modules of type 1 the module that showed the lowest failure load and deflection (3,440 Pa/43 mm) remained with an intact rear glass after failure. Modules of type 2 failed at 6210 ± 380 Pa with a deflection of 87 ± 4 mm. Results in a similar range could be observed on module types 3 with 6,220 ± 460 Pa at 85 ± 11 mm and type 4 with 6,000 ± 360 Pa at 90 ± 2 mm. Similar to type 1, one of five modules of type 3 remained with an intact rear glass and showed significantly lower failure loads than the rest of this type (4,280 Pa / 67 mm). The reason for these reduced failure loads could not conclusively be evaluated in the scope of this work. It is assumed to be related to the statistically scattering of the bending strength.

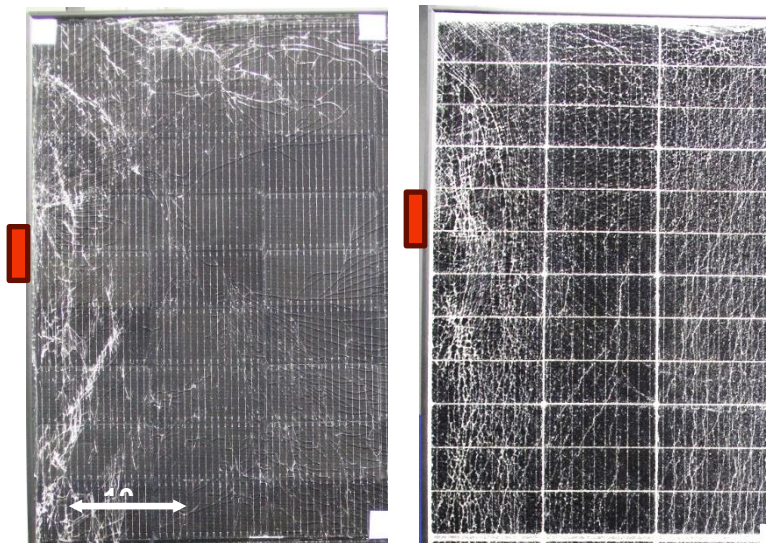**Figure 9**. Representative breakage patterns shown on 1/4 of modules after ML tests until *failure in pressure direction, clamping positions sketched as red squares; Left: Representative for types 1 to 3; Right: Representative for type 4.*

The ML tests resulted in glass breakage patterns as exemplarily shown in Figure 9. In accordance with descriptions from literature [8], modules of type 4 with 3.2 mm and residual

surface stresses in the range of TTG acc. to EN 12150-1 (≤ -90 MPa) showed a fine grained fracture pattern (Figure 9, right). Module types 1 to 3 showed a coarser fracture pattern with large unbroken pieces, long cracks (Figure 9, left) and could therefore qualitatively be classified into a lower residual surface stress range, which is consistent with the results of the SCALP measurements. The majority of breakage patterns showed fracture origins in the clamping regions , which is consistent with results from FEM simulations in section 3.3 and reported maximum stresses on PV modules under load from Romer et al. [10].

To assess the potential influence of the frame height in relation to the significantly reduced failure loads of module type 1, mechanical simulations with the method of finite elements (FEM) were conducted, as described in chapter 3.3.

3.3. Finite Element Analyses

The goal was to investigate the influence of the frame height of module designs with different glass thicknesses (as partly tested, cf. Table 3), and thereby occurring maximum first principal stress. For the simulations a previously published FEM model [11, 12] was adapted to simulate the tested PV module types. Subsequently, load simulations with 30 mm and 35 mm frame heights for glass/glass modules with 2.0 mm (type 1) and 1.6 mm (type 2 and 3) as well as for glass-backsheet modules with a 3.2 mm glass thickness (type 4) were conducted. In order to study the influence of only the frame height and glass thickness, all other parameters such as the module dimensions (1,722 x 1,134 mm^2) and material properties remained constant for all variations. Also, for all variations the same frame design from [11] was used, where the lower part of the frame is stretched for the 35 mm frame height. The surface pressure load was 6,000 Pa. Table 3 shows the simulated module variations.

Table 3. Simulated module variations.

Design	Glass thickness / mm	Frame height / mm	Module type
Glass/glass	2.0 / 2.0	35	1 (tested, simulated)
Glass/glass	2.0 / 2.0	30	simulated
Glass/glass	1.6 / 1.6	35	simulated
Glass/glass	1.6 / 1.6	30	2 (tested, simulated)
Glass/backsheet	3.2	35	simulated
Glass/backsheet	3.2	30	4 (tested, simulated)

Figure 10 depicts the simulated first principal stress on the front surface (towards the encapsulation) of the rear pane, which corresponds to the tensile stress equivalent, exemplarily for module type 1 (left figure) along with the maximum first principal stress values for all considered parameter variations (right figure).
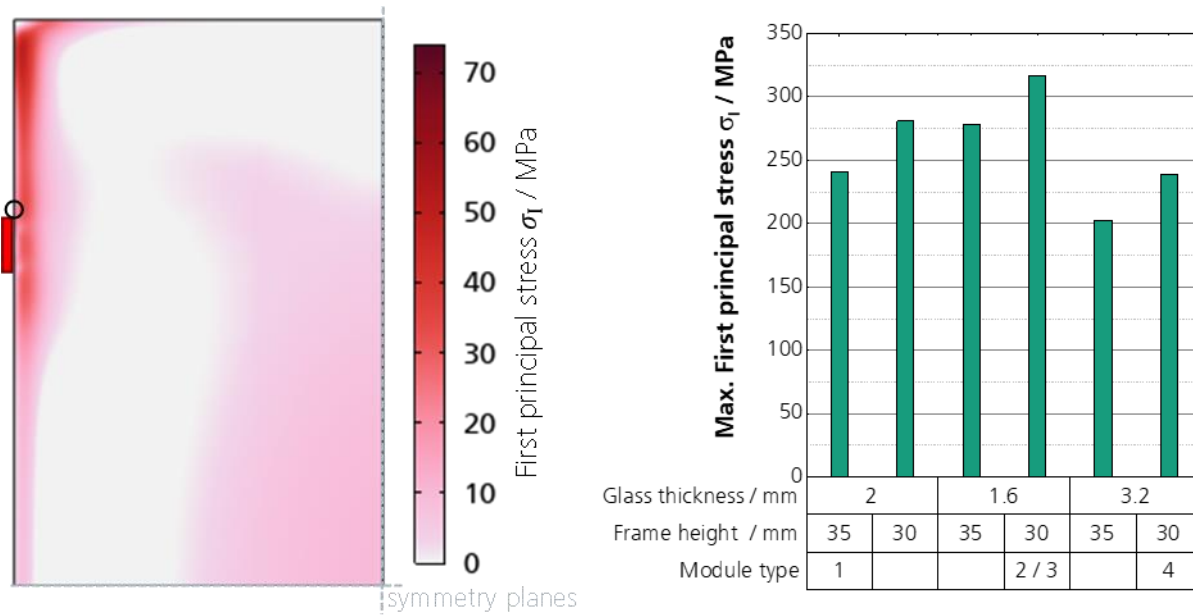
Figure 10. Left: Distribution of simulated first principal stress on top side of the rear pane (towards the encapsulation) of ¼ of module type 1 with a surface pressure load of 6,000 Pa. The position of the clamping is indicated by a red box and position of maximum stress is indicated by the black circle; Right: Maximum first principal stress in front and rear pane at surface pressure load of 6,000 Pa for all simulated variations. Note: The absolute stress values are exaggerated by singularities. But, the tendency is correctly represented, which was the purpose of these simulations.

The simulation results indicate that the maximum stress at the panes generally occur in a very small area directly at the glass edge next to the clamping position towards the module corner. This is due to a high curvature around the clamping position, as was shown by [10]. The higher stress values in the area from the clamping position to the module corner correspond very well to areas, where a severe fracture pattern could be observed after the ML experiments (compare Figure 9). Furthermore, the higher stress in the module center is conform to a higher fracture intensity observed at these locations.

By analyzing the maximum stress values for the different simulated module variations, it can be observed that the mechanical stability of the module is enhanced by an increased frame height as well as an increased glass thickness. A higher frame increases the bending resistance and hence, decreases the curvature of the glass pane around the clamping position. Similarly, the bending resistance of glass is enhanced by increasing its thickness. Moreover, the variation equivalent of module type 1 (with a frame height 30 mm) results in a significantly lower maximum first principal stress compared to the variation of module types 2/3. This could imply a higher mechanical stability and consequently, an increase of the failure load.

4. Conclusion

Increasing glass surface stresses coincide with increasing characteristic bending strengths of panes. Furthermore, the SCALP measurement method can reliably be used for the determination of the surface glass stress on PV modules. A surface texture as well as an anti-reflection coating on the glass surface resulted in reduced values for the residual surface stress compared to similar samples without a surface texture and coating. This observation needs to be further investigated.

Results on four different commercially available module types indicate the use of glass qualities with different degrees of prestressing of the PV module front and rear panes, also when similar thicknesses are used. Especially the higher surface prestressing in panes with 1.6 mm thickness compared to 2.0 mm is an interesting result, since the prestressing in the

tempering process becomes generally more complex and challenging with thinner glass [13]. Module type 1 with two glasses, each 2.0 mm thick and the lowest prestressing showed significantly reduced failure loads and deflections for all the investigated module types. This suggests that the residual surface stress could be one important indicating parameter regarding the general module stability.

An eventual influence of the frame height in this sense was investigated with FEM simulations of the different module types under a pressure load up to 6,000 Pa. The results reveal a decrease in first principal stress in the panes with increasing frame height. This suggests that the reduced failure loads observed in module type 1 might be dependent on the glass quality. However, the glass edge strength – as one main quality parameter – is predominantly determined by the processing and has a significant influence on the breakage behavior of the glass elements.

The similar deflection behavior of modules with 2 x 1.6 mm and modules with 3.2 mm panes can be explained by a similar overall laminate thickness, resulting in an overall similar stiffness, if full bonding can be assumed.

The visual assessment of the breakage patterns allowed a general qualitative classification between modules with TTG and panes with glass qualities significantly below TTG. In accordance with simulations from Romer et al. [10], fracture origins could be identified in the clamping regions on the front pane, where the simulations showed maximum stresses during pressure load application.

It must be noted that modules in this work were tested with idealized homogeneous pressure load profiles. However, stability of modules with thinner panes might appear different, when scenarios closer to reality with inhomogeneous loads as standardly happen in field exposition are considered. These could lead to more complex load distributions e.g., with torsional loads and maximum stresses exceeding those appearing during homogeneous load cases. Especially in the context of the ongoing trend towards using larger modules with decreasing glass thicknesses, the influence of the compressive glass surface stress could become a more dominant parameter for the module stability under realistic load conditions.

Data availability statement

The raw data of the results shown in this study are available from the corresponding author, J. Markert, upon reasonable request.

Underlying and related material

Not applicable.

Author contributions

Conceptualization, J. Markert, and F. Ensslen; methodology, J. Markert, E. Job, A. Beinert and T. Rist ; formal analysis, J. Markert; data curation, J. Markert and A. Beinert; writing—original draft preparation, J. Markert, F. Ensslen, and A. Beinert; writing—review and editing, J. Markert, F. Ensslen, A. Beinert, I. Hädrich and D. Philipp; visualization, J. Markert; supervision, I. Hädrich and D. Philipp; project administration, J. Markert; funding acquisition, D. Philipp. All authors have read and agreed to the published version of the manuscript.

Competing interests

Not applicable.

Funding

Acknowledgement

References

[1]   ITRPV, "International Technology Roadmap for Photovoltaic (ITRPV): 2022 Results," 2023.

[2]   P. Sinha and A. Wade, "Assessment of Leaching Tests for Evaluating Potential Environmental Impacts of PV Module Field Breakage," IEEE J. Photovoltaics, vol. 5, no. 6, pp. 1710–1714, 2015, doi: 10.1109/JPHOTOV.2015.2479459.

[3]   A. Sinha et al., "Glass/glass photovoltaic module reliability and degradation: a review," J. Phys. D: Appl. Phys., vol. 54, no. 41, p. 413002, 2021, doi: 10.1088/1361-6463/ac1462.

[4]   M. Köntges, S. Kurtz, C. Packard, U. Jahn, K. A. Berger, and K. Kato, Performance and reliability of photovoltaic systems: Subtask 3.2: Review of failures of photovoltaic modules : IEA PVPS task 13 : external final report IEA-PVPS. Sankt Ursen: International Energy Agency Photovoltaic Power Systems Programme, 2014. [Online]. Available: https://edocs.tib.eu/files/e01fb16/856979287.pdf

[5]   M. Aghaei et al., "Review of degradation and failure phenomena in photovoltaic modules," Renewable and Sustainable Energy Reviews, vol. 159, p. 112160, 2022, doi: 10.1016/j.rser.2022.112160.

[6]   DIN EN ISO 1288-3, 1288-3:2007, DIN Deutsches Institut für Normung e. V. (DIN), Berlin, Oct. 2007.

[7]   DIN EN 1288-5: Glas im Bauwesen - Bestimmung der Biegefestigkeit von Glas: Teil 5: Doppelring-Biegeversuch an plattenförmigen Proben mit kleinen Prüfflächen, DIN Deutsches Institut für Normung e.V., Sep. 2000.

[8]   E. Wagner, Glasschäden: Oberflächenbeschädigungen, Glasbrüche in Theorie und Praxis, 5th ed. Stuttgart: Fraunhofer IRB Verlag, 2020.

[9]   ISO 12491: Statistical methods for quality control of building materials and compionents, ISO, May. 1997.

[10] P. Romer, K. B. Pethani, and A. J. Beinert, "Effect of inhomogeneous loads on the mechanics of PV modules," Prog. Photovolt: Res. Appl., 2023, doi: 10.1002/pip.3738.

[11] A. J. Beinert, P. Romer, M. Heinrich, M. Mittag, J. Aktaa, and H. Neuhaus, "The Effect of Cell and Module Dimensions on Thermomechanical Stress in PV Modules," IEEE J. Photovoltaics, vol. 10, no. 1, pp. 70–77, 2020, doi: 10.1109/JPHOTOV.2019.2949875.

[12] A. Tummalieh, A. J. Beinert, C. Reichel, M. Mittag, and H. Neuhaus, "Holistic design improvement of the PV module frame: Mechanical, optoelectrical, cost, and life cycle analysis," Prog. Photovolt: Res. Appl., vol. 30, no. 8, pp. 1012–1022, 2022, doi: 10.1002/pip.3533.

[13] B.-W. Fan, K.-Q. Zhu, Q. Shi, T. Sun, N.-Y. Yuan, and J.-N. Ding, "Effect of glass thickness on temperature gradient and stress distribution during glass tempering," Journal of Non-Crystalline Solids, vol. 437, pp. 72–79, 2016, doi: 10.1016/j.jnoncrysol.2016.01.008.